

Supplementary Material

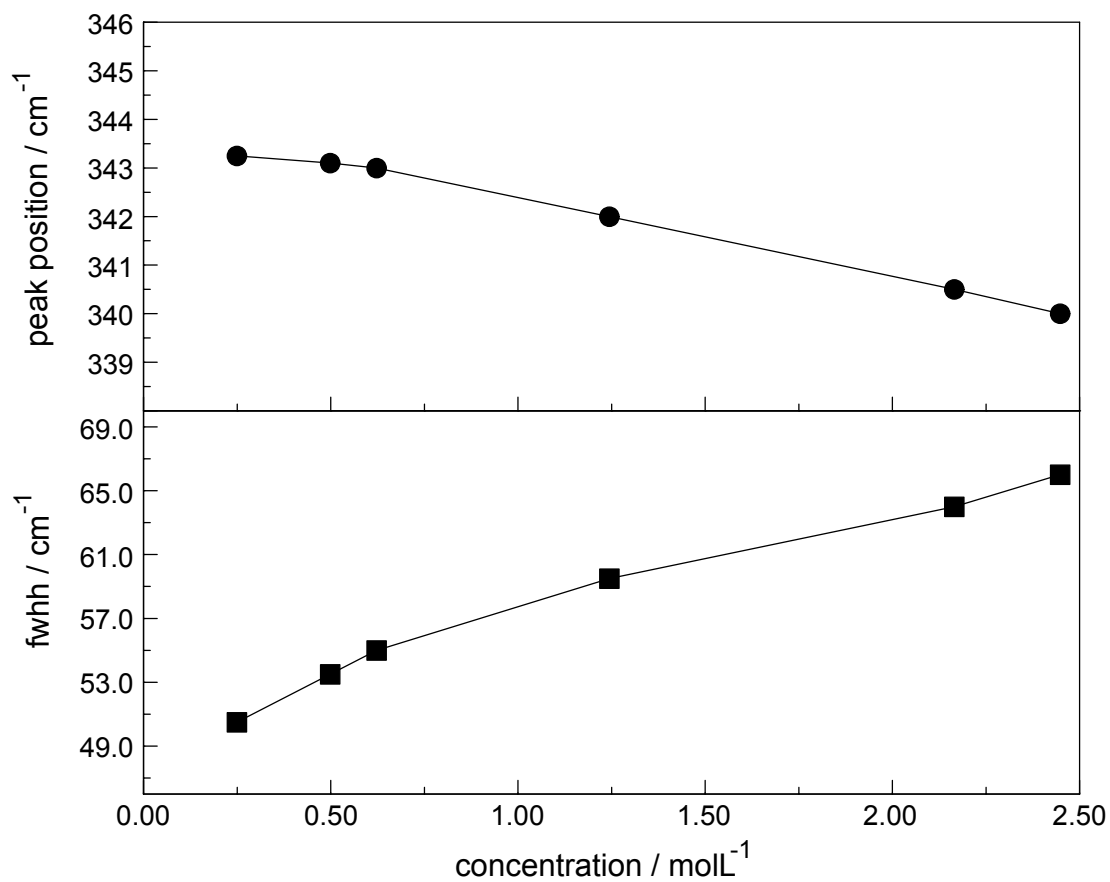


Figure S1. Concentration effects on the ν_1 La-O mode in $\text{La}(\text{ClO}_4)_3(\text{aq})$ at 23 °C. A: peak position (cm^{-1}) and B: fwhh (cm^{-1}).

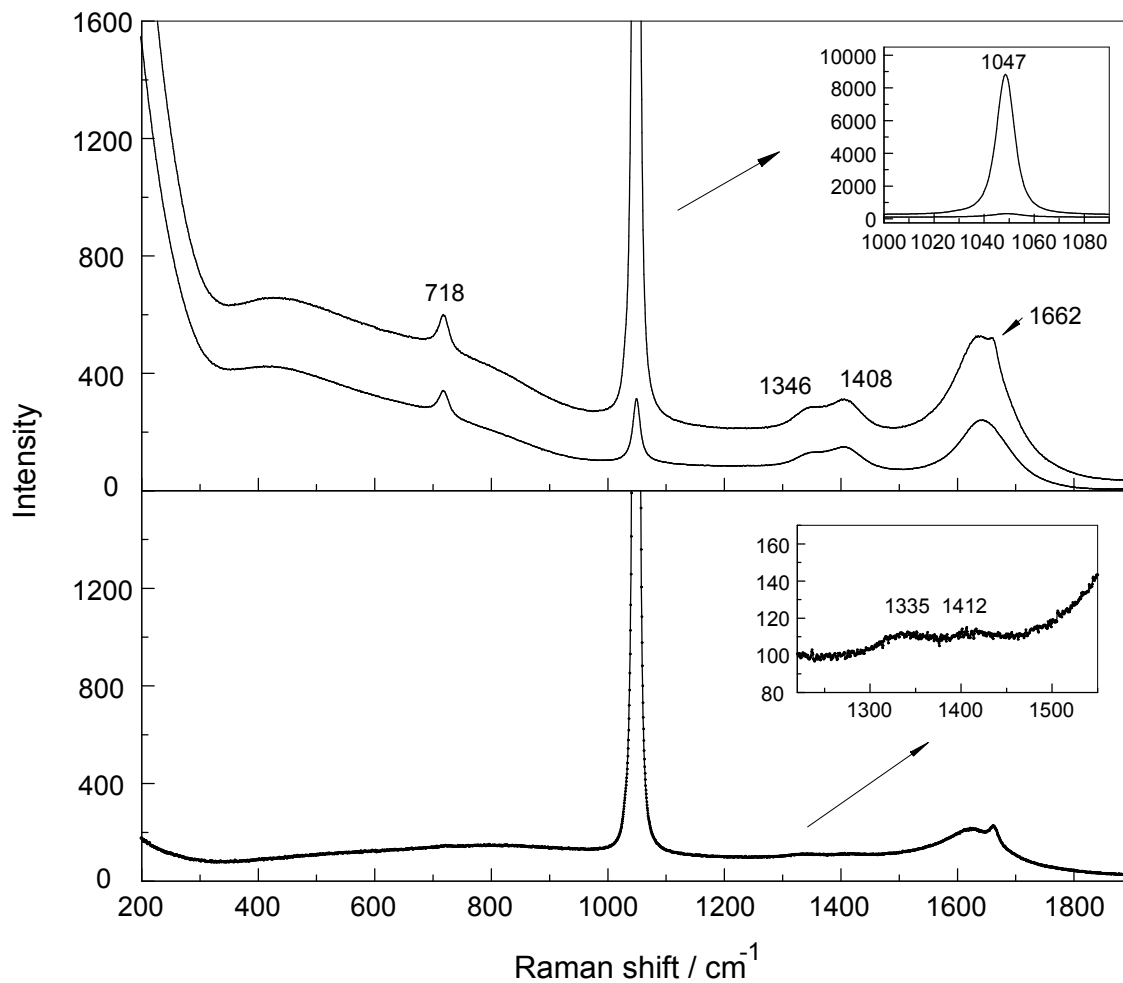


Figure S2. Overview Raman spectrum of a $0.409 \text{ molL}^{-1} \text{ NaNO}_3(\text{aq})$ in the polarized and depolarized scattering (upper panel) and isotropic scattering (lower panel). The three Raman active modes of $\text{NO}_3^-(\text{aq})$ are shown: at 718 cm^{-1} the depolarized bending mode, $\nu_4(e'')$; at 1047.62 cm^{-1} the symmetric N-O stretch, $\nu_1(a_1')$, a strongly polarized band (depolarization degree = 0.034) which appears in the isotropic scattering; the broad and weak double band $\nu_3(e')$ at 1347 and 1408 cm^{-1} (slightly polarized) and the overtone of $\nu_2(a_2'')$ (only infrared active), $2\nu_2$ at 1662 cm^{-1} which is polarized and appears also in the isotropic scattering. Note the broad band at 1637 cm^{-1} (polarized scattering) which is due to the water bending mode. Furthermore, very broad, weak bands appear between 300 and 900 cm^{-1} which are due to the librational modes of water. It should be noted that the $\text{NO}_3^-(\text{aq})$ bands are slightly concentration dependent. The $\nu_1(a_1')$ stretching band has the following band parameters at infinite dilution (extrapolation of the spectroscopic parameters to zero concentration: peak position = 1047.3 cm^{-1} and $\text{fwhh} = 6.55 \text{ cm}^{-1}$ (slit width used 0.7 cm^{-1}). The peak position for $\nu_4(e'') = 717.5 \text{ cm}^{-1}$ and $\text{fwhh} = 15.8 \text{ cm}^{-1}$.

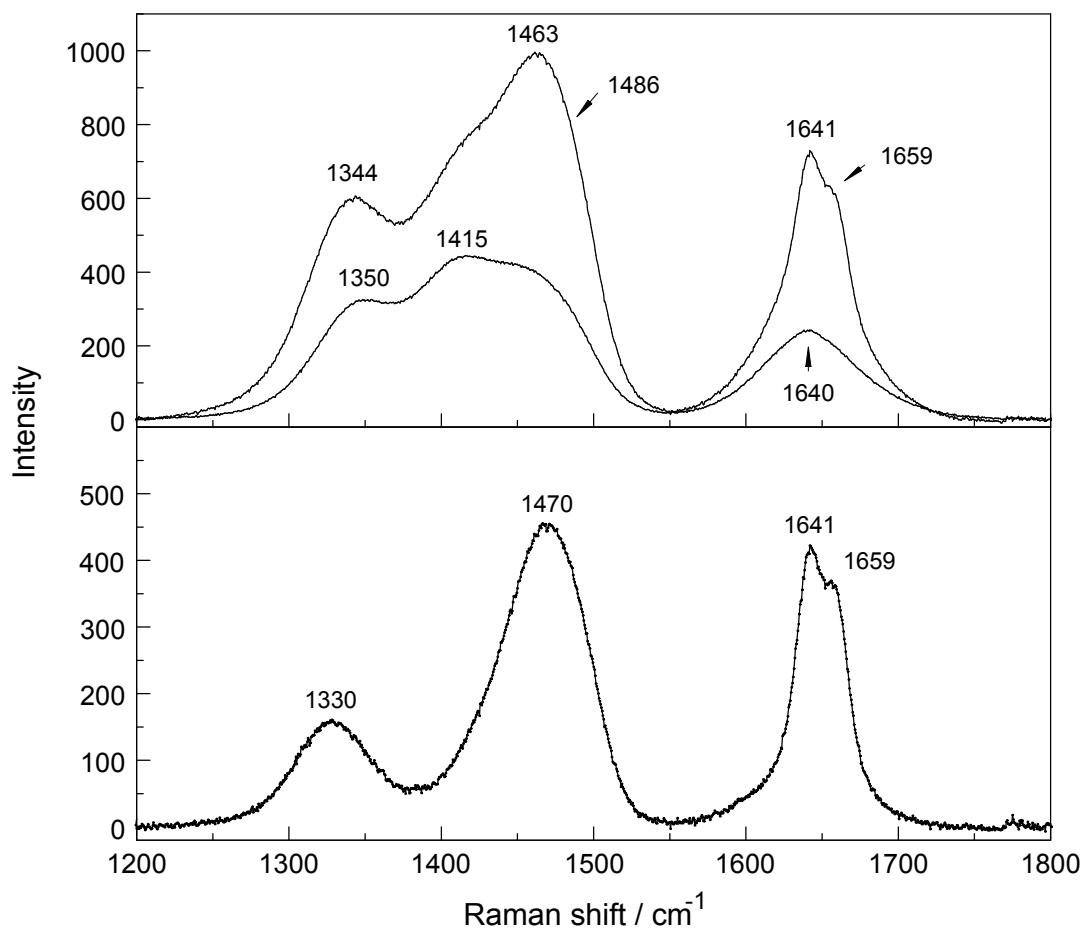


Figure S3. Raman spectra of a $1.844 \text{ mol L}^{-1} \text{ La}(\text{NO}_3)_3(\text{aq})$ in the region of the $\nu_3(\text{e}')$ bands. The upper panel shows the polarized and depolarized scattering contributions while the lower panel shows the isotropic scattering. Note the complicated band profile of the $\nu_3(\text{e}')$ mode in the polarized scattering. The bands at $1641 \text{ (fwhh} = 24.6 \text{ cm}^{-1}\text{)}$ and at $1659 \text{ cm}^{-1} \text{ (fwhh} = 22.1 \text{ cm}^{-1}\text{)}$ are due to the overtone of $\nu_2(\text{a}_2'')$, which is normally only active in the infrared. The narrow band at 1641 cm^{-1} is due to the NO_3^- in the nitrato-complex while the second narrow band is due to the unligated nitrate ($2\nu_2$ at 1662 cm^{-1} for $\text{NO}_3^-(\text{aq})$). Both bands are polarized. Furthermore, the small broad band at 1640 cm^{-1} in the depolarized scattering is due to the water deformation mode in this concentrated solution. (The water deformation band is completely overlapped by the overtones of $\text{NO}_3^-_{\text{free}}$ (1659 cm^{-1}) and $\text{NO}_3^-_{\text{bound}}$ at 1641 cm^{-1} .) In the isotropic scattering, two separated broad bands at 1330 cm^{-1} and 1470 cm^{-1} are due to the antisymmetric stretching mode, $\nu_3(\text{e}')$. Both bands appear not symmetrical and contain unresolved component bands.

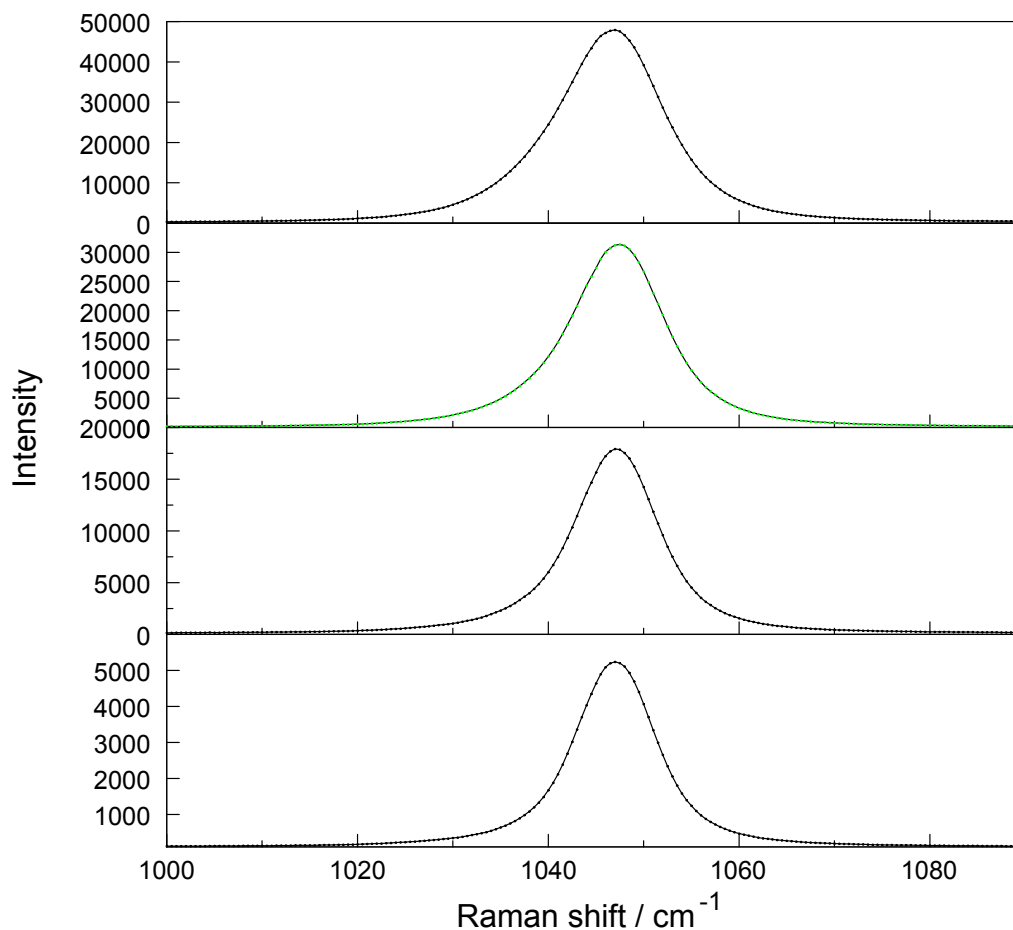


Figure S4. Isotropic Raman scattering profiles of the symmetric N-O stretch, $\nu_1(a_1')$ of four aqueous $\text{La}(\text{NO}_3)_3$ solutions; from top to bottom: 1.844, 1.050, 0.466 and 0.121 molL⁻¹ in solute concentration. In the 1.844 molL⁻¹ $\text{La}(\text{NO}_3)_3(\text{aq})$ the $\nu_1 \text{NO}_3^-$ stretching mode appears at 1050.0 cm⁻¹ as a broad and asymmetric band due to extensive nitrato-complex formation while the $\nu_1 \text{NO}_3^-$ (aq) in very dilute solution appears at 1047.5 cm⁻¹.

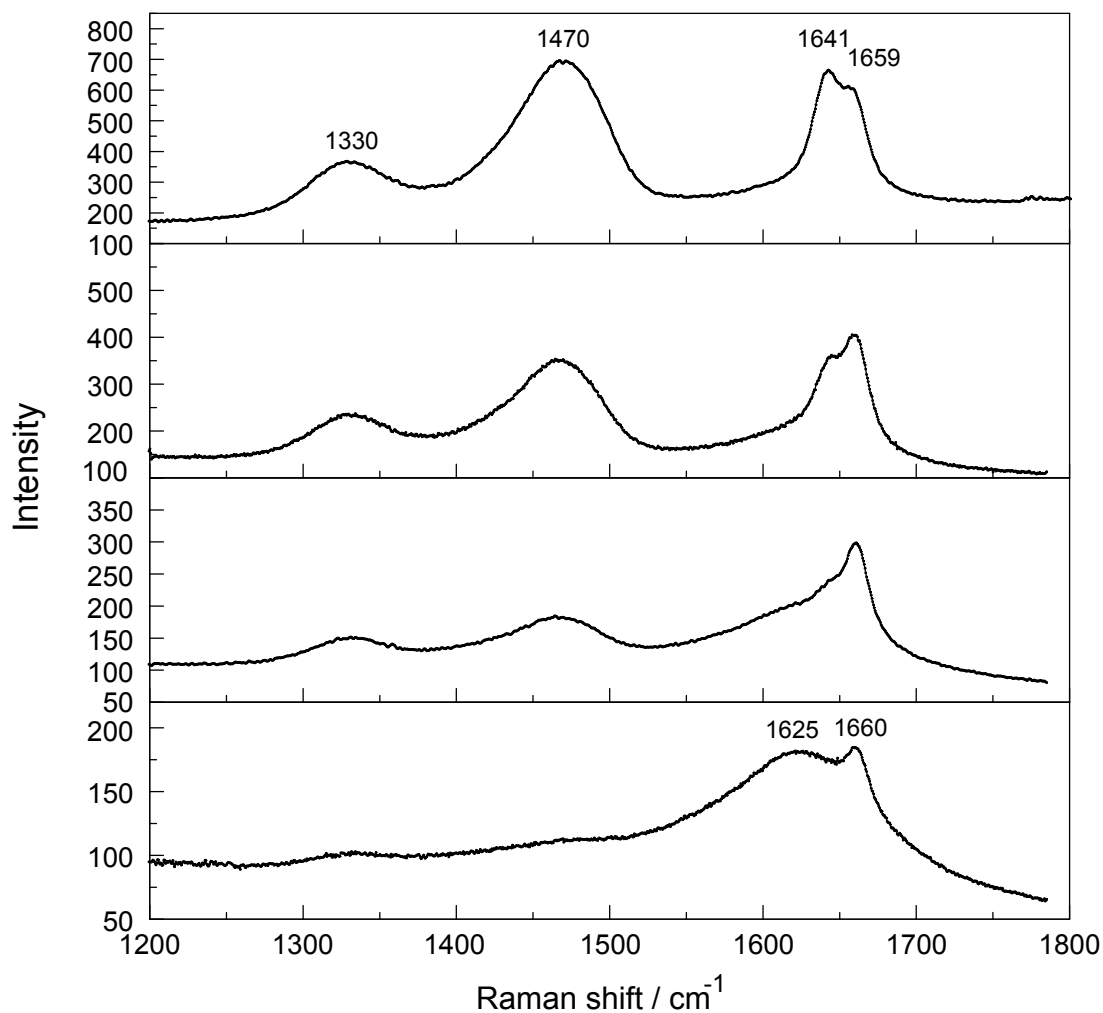


Figure S5. Isotropic Raman scattering profiles from 1200 – 1800 cm^{-1} of four aqueous $\text{La}(\text{NO}_3)_3$ solutions; from top to bottom: 1.844, 1.050, 0.466 and 0.121 molL^{-1} in solute concentration. Note, with dilution the the broad scattering contributions (anti-symmetric stretching motion, $\nu_3(e'')$) at 1330 cm^{-1} and 1470 cm^{-1} are vanishing as well as the overtone $2\nu_2$ at 1641 cm^{-1} . In the 0.121 molL^{-1} $\text{La}(\text{NO}_3)_3(\text{aq})$ these contributions are almost disappeared while the very broad water deformation band at 1625 cm^{-1} becomes the strongest band. It should be pointed out that the water deformation band is with $\sim 120 \text{ cm}^{-1}$ much broader than the $2\nu_2 \text{ NO}_3^-$ bands (bound and free) and this is the reason that the overtone modes are easily detectable in these solutions. The mode at 1660 cm^{-1} due to the overtone $2\nu_2 \text{ NO}_3^-(\text{aq})_{\text{free}}$ is still observable in the isotropic spectrum (compare the results in $\text{NaNO}_3(\text{aq})$ in Figure S2 and the explanation in the Figure caption).

Table S1. Results for $[\text{La}(\text{OH}_2)_9]^{3+}$ in the gas phase and with a polarizable continuum (PC model) applying Hartree-Fock (HF) and B3LYP calculations with the mixed basis set LANL2DZ for La^{3+} and 6-31G for O and H for the $[\text{La}(\text{OH}_2)_9]^{3+}$ and alternatively with the basis set with 6-31G(d,p) with polarization functions.

Method/basis set	ν_1 (cm^{-1})	La – O (\AA)	O – H (\AA)	H-O-H ($^\circ$)	energy (a.u.)
HF/ 6-31G, LANL2DZ	292.9	2.65 2.64	0.96	110.4	-714.296
HF/ 6-31G(d,p), LANL2DZ	281.9	2.67 2.65	0.95	106.1	-714.545
B3LYP/6-31G, LANL2DZ	297.5	2.62 2.60	0.98	109.6	-718.239
B3LYP/6-31G(d,p), LANL2DZ	287.3	2.63 2.62	0.97	105.6	-718.441
B3LYP/6-31G, LANL2DZ solv.(PCM)	328.2	2.58 2.56	0.99	110.2	-718.865
B3LYP/6-31G(d,p), LANL2DZ solv. (PCM)	321.0 *	2.59 2.57	0.98	106.6	-719.065

* optimized structure with two imaginary vibrations

Comparison of some results of calculations with mixed basis sets LANL2DZ for La^{3+} and 6-31G for O and H as well as 6-31G(d,p).

Using the same basis sets, the symmetric La-O stretch frequency is about 5 cm^{-1} higher using the B3LYP functional in comparison with the HF method. The frequency is downshifted by about 10 cm^{-1} if polarization functions were added. The strongest effect with a frequency upshift of about 30 cm^{-1} , however, and a better agreement with the experimental frequency value is obtained by embedding the nona-hydrate in the polarizable water continuum (PC model). In this case also the La-OH₂ average bond distance agrees more closely with the experimental ones. (Because the optimized structure of the last calculation in the Table showed imaginary vibrations, we used in this study the results of the B3LYP calculations with LANL2DZ, 6-31G basis sets).

Table S2. DFT frequencies at the B3LYP/ LANL2DZ/ 6-31G level of theory for the nona-hydrate of Ln³⁺, [Ln(H₂O)₉]³⁺ with a solvation shell (PC model).

freq./ cm ⁻¹	Sym- metry	Assign- ment	Intensity	freq./ cm ⁻¹	Sym- metry	Assign- ment.	Intensity	freq./ cm ⁻¹	Sym- metry	assign- ment	intensity	freq./ cm ⁻¹	Sym- metry	Assign- ment	Intensity
36.9	e	LaO ₉	0.06	239.9	a ₂	τ,ω	0.06	362.2	a ₁	τ,ω	17.1	1600.6	a ₁	δ	9.8
64.9	e	LaO ₉	0.37	239.9	a₁	LaO ₉	0.02	377.3	a ₂	ω	0.00	3434.3	e	v _s	58.2
79.3	a₂	LaO ₉	0.02	256.4	e	τ,ω LaO ₉	0.60	474.1	a ₂	ρ	1.1	3434.6	e	v _s	112.3
85.2	a₁	LaO ₉	0.27	264.2	e	τ,ω/ LaO ₉	1.76	485.9	e	ρ	0.40	3435.2	a ₁	v _s	37.2
97.1	a₁	LaO ₉	5.26	282.5	e	τ	2.2	495.0	a ₁	ρ	2.4	3438.7	a ₂	v _s	0.46
109.7	e	LaO ₉	0.66	287.5	e	LaO ₉ / ω	1.74	524.6	e	ρ	4.0	3439.5	e	v _s	17.5
111.0	a₂	LaO ₉	0.03	289.1	a₂	LaO ₉ / ω	0.03	542.7	a ₂	ρ	0.01	3452.0	a ₁	v _s	1487.3
115.4	e	LaO ₉	0.06	302.1	a ₂	ω	0.00	548.7	e	ρ	3.6	3526.9	a ₂	v _{as}	0.75
122.8	a₂	LaO ₉	0.04	310.1	e	ω	10.5	1579.0	a ₁	δ	10.5	3527.0	a ₁	v _{as}	135.9
124.4	e	LaO ₉	0.13	328.2	a₁	LaO ₉	1.35	1579.8	e	δ	13.0	3527.0	e	v _{as}	116.4
195.8	a ₁	τ	6.6	333.3	e	ω	0.20	1584.2	e	δ	5.5	3527.2	e	v _{as}	66.1
211.0	e	τ	1.0	342.4	a ₁	ω	4.3	1587.8	a ₂	δ	0.88	3528.9	e	v _{as}	98.9
227.7	e	τ	6.0	350.8	e	τ	12.3	1593.9	e	δ	3.8	3529.0	a ₂	v _{as}	0.26

The LaO₉ skeletal vibrations are printed in bold letters. Note the breathing vibrational frequency of the cluster at 328.2 cm⁻¹. The notations of the water vibrations are: v_s: symmetric stretching, v_{as}: antisymmetric stretch, δ: deformation, ρ: rocking, ω: wagging, τ: twisting.

Table S3. Raman and infrared data on $\text{NO}_3^-(\text{aq})$ of a $0.409 \text{ mol}\cdot\text{L}^{-1} \text{ NaNO}_3(\text{aq})$ at $23 \text{ }^\circ\text{C}$. The Raman spectrum is given in Figure S2.

normal mode	Raman				infrared
	peak position	I_{rel}	fwhh	Depol. ratio	
$\nu_4(\text{e}')$	718	3.8	17.8	dp	718 *
$\nu_2(\text{a}_2'')$	-	-	-	-	832
$\nu_1(\text{a}_1')$	1047.62	100.0	7.08	0.034	-
$\nu_3(\text{e}'')$	1346/1408	14.0	56/56	0.72	1352/1406
$2 \times \nu_2(\text{a}_1')$	1662	1.98	21	0.5	-

- extremely weak band

Table S4. Band fit results for the ν La-O stretching band into two component bands at 314 cm^{-1} and 343 cm^{-1} for $\text{La}(\text{NO}_3)_3(\text{aq})$ at 23 $^\circ\text{C}$.

Concentration / $\text{mol}\cdot\text{L}^{-1}$	R_w (mol ratio $\text{H}_2\text{O}/\text{La}(\text{NO}_3)_3$)	314 cm^{-1} - band		343 cm^{-1} - band		α	Q_1
		A_{314}	Fwhh / cm^{-1}	A_{343}	Fwhh / cm^{-1}		
1.844	26.09	1980	49	2548	57	0.44	0.76
1.050	49.1	1773	49	3668	53	0.33	0.70
0.466	115.26	888.5	50	3287	53	0.21 ₅	0.75
0.121	455.3	167	50.6	1195	52	0.12	1.28